

---

## The design of gridshells with torsion free layout and planar quads made simple

Cyril DOUTHE\*, Romain MESNIL<sup>a</sup>, Olivier BAVEREL<sup>a</sup>

\*Laboratoire Navier, Ecole des Ponts Paris Tech, Univ. Gustave Eiffel, CNRS  
6&8 avenue Blaise Pascal, 77420 Champs sur Marne, France  
cyril.douthe@univ-eiffel.fr

### Abstract

Connection nodes are usually the costliest elements of gridshells because of their geometrical complexity. Their fabrication might be significantly simplified if they have no geometrical torsion. Architectural geometry literature has therefore focused on developing geometrical structures with null torsion, such as conical and circular meshes, and on associated generation methods. These meshes are closely linked with principal curvature and therefore give limited freedom to the designer. This paper investigates an alternative approach based on the theory of parallel transformation to define a torsion free layout on any planar quadrilateral mesh. An exact construction method of the corresponding linear space is presented as well as an approximate method using the Kangaroo solver. It proposes then a strategy to build nodal axes so that they fit with surface normals. This strategy is evaluated from a geometrical and mechanical point of view through different mesh examples. Their performances are compared with a trivial technical solution with geometrical torsion at nodes where beam mid-planes are chosen perpendicular to the surface. Finally, the authors conclude on the influence of such design choices made on geometrical criteria for the beam layout on the global mechanical behaviour of gridshells.

**Keywords:** Architectural Geometry, Planar Quad meshes, Torsion free nodes, gridshell, Structural Analysis

### 1. Introduction

Gridshells are popular structures, as they allow to elegantly cover relatively wide spans with limited weight while ensuring transparency. Their geometry usually has double-curvature, which gives them shape resistance. However, they are often built with straight beams and flat panels to reduce costs. Because of panel planarity, the Gaussian curvature of the envelope is located only at connection nodes between members: nodes concentrate the geometrical complexity of the structure and are therefore the most complex element to manufacture. However, their fabrication might be significantly simplified if they are torsion-free, i.e. if the beam mid-planes meet on a common axis (cf. figure 1).

A common constraint on the node axes is their approximate orthogonality to the surface. This is due to the fact that, for fabrication and structural purposes, it is desirable that beam top faces are approximately parallel to the surface. Otherwise, i) large kinks occur between beams and panels (a problem explored in [1]), ii) beams are poorly oriented to withstand wind loads on the envelope and iii) the structure transparency is decreased. As a consequence, not any parallel mesh is suitable to define node axes.

For a given mesh, it is always possible to set a gridshell geometry with torsion free nodes by setting all the axes with the same orientation (for example vertical). This approach gives torsion-free nodes, but generally the node orientations poorly satisfy the three constraints mentioned above. Non-constant axes

can also be found for some remarkable surfaces like revolution surfaces but in the general case, it is often necessary to get insight on the differential geometry of the grid and surface.

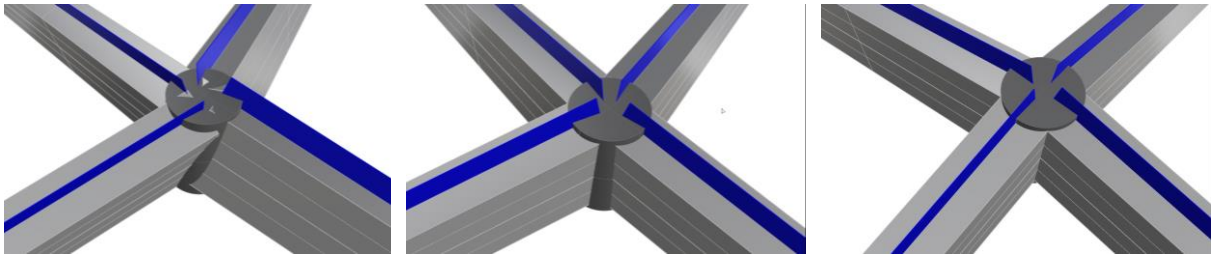


**Figure 1:** Beam layouts with constant beam height : (left) normal layout with torsion at node and gaps of bottom layout, (middle) torsion free layout with gaps of bottom layout, (right) edge offset mesh with torsion free layout and perfect alignment of layers.

In the case of meshes with planar faces, Pottmann *et al.* showed in [2] the equivalence between having torsion-free nodes and the existence of a parallel mesh: a mesh in which all the edges and faces are parallel to the mesh, but with different edge lengths. The parallel meshes to a given mesh form a linear space. The dimension of this space depends mostly on the pattern (and to a lesser extent on boundary conditions). For triangular meshes, the only parallel transformations are homotheties. Then, the space of parallel transforms becomes richer and richer as the average number of edges per face increases (quadrangular, hexagonal) [3].

Hence, due to the dimension of parallel mesh spaces, most triangle meshes cannot be covered by torsion-free nodes with axes normal to the surface, while it is always possible for hexagonal meshes. For quadrangular meshes, one can find proper nodes as long as the edges approximate the principal curvature directions of the underlying arbitrary smooth surfaces: these are the only lines along which the surface normal undergoes no geometrical torsion. Pottmann *et al* have indeed shown that the two dual families of planar quad meshes that approximate curvature lines are circular and conical meshes [4].

For a given surface however, principal curvature directions are imposed and can be unsuitable for design purposes. For example, Pottmann *et al* shows the curvature lines on the roof of the Visconti court in Le Louvres, designed by architects Rudy Ricciotti and Mario Bellini [5]. The configuration is badly suited for a gridshell: there is a high variation in the size and aspect ratio of faces, beams have a poor mechanical alignment, and the pattern with its four singularities is subjectively unesthetic. Consequently, a hybrid triangular and quadrangular pattern was chosen for the final structure. This hybridization strategy is one among many like for example the caravel method developed in [6].

Many questions arise then for the designer who would like to deviate from principal curvature directions and to prescribe the grid layout on the surface. Would it be possible to define an offset which is not normal to the surface but tends toward this normal? To what extent this deviation from surface normal will influence the mechanical behaviour of the structure? This article addresses these two questions in a relatively pragmatic approach in order to provide a set of practical solutions for structural design and to enlarge the possible design spaces. Section 2 investigates how a torsion-free layout can yield node axes that fit at best the surface normals. The method is based on the linear space of parallel transformations and projection on admissible sub-spaces. An evaluation of maximum deviation to normal with differential geometry is also proposed. The whole is illustrated in a practical example. Section 3 develops practical implementation aspects in the framework of a Pavilion case study [7]. In particular, the influence of the beam layout on the structural behaviour of the gridshell is investigated.

## 2. Optimizing torsion-free beam layout for alignment with surface normals

In this section, we study thus practical fabrication constraints and evaluate their relation to particular meshes. We build upon the now well-known design space offered by parallel mesh transformations, which have been described in [2] and extended to the design of nexorades in [8].

## 2.1 Parallel meshes

Discrete offsets satisfy two conditions: the beams are planar and they all meet along a common axis. This condition can be written as a linear system of equations, as already mentioned by [4, 9], who explored the potential offered by the design space of parallel transformations for mesh modelling. Figure 2 represents a torsion-free beam layout constructed from two parallel meshes  $M$  and  $M'$ . The edges of the meshes  $M$  and  $M'$  are parallel, and thus coplanar, therefore, the support structure (shaded blue region) is planar and without torsion.

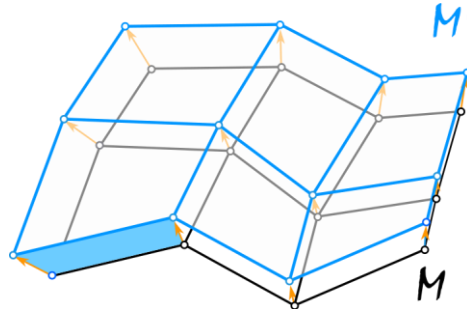


**Figure 2:** Discrete offset direction (orange arrows) can be defined from two parallel meshes  $M$  and  $M'$ . The support structure consists of planar sections

We write  $\mathbf{X}$  the nodal displacement between two parallel meshes (i.e. the differences between the vertices of  $M$  and  $M'$ , which is represented with orange arrows in Figure 2), there exists a matrix  $\mathbf{A}$  so that equation (1) is verified.

$$\mathbf{A} \cdot \mathbf{X} = \mathbf{0} \quad (1)$$

A lower bound for the dimension  $d$  of the design space is given in [4] and it has been estimated for several common structural patterns in [3], leading to a classification of patterns for gridshell structures.

$$d \sim n_E - \sum_{i=1..n_F} (n_E^i - 2) \quad (2)$$

(where  $n_E$  is the total number of edges in the mesh and  $n_E^i$  is the number of edges in face  $i$ ). In practice, for a PQ mesh with  $n_F$  faces, the number of degrees of freedom is approximately proportional to  $\sqrt{n_F} \sim 2n_E$ . The design space is thus rather small. An orthonormal basis  $\mathbf{N} \in \mathbb{R}^{3n_V, d}$  of  $\mathbf{A}$  can be found so that any vector  $\mathbf{X}$  can be written as  $\mathbf{X} = \mathbf{N}\mathbf{W}$ , with  $\mathbf{W} \in \mathbb{R}^d$

$$\mathbf{A} \cdot \mathbf{X} = \mathbf{0} \Leftrightarrow \mathbf{X} = \mathbf{N}\mathbf{W} \quad (3)$$

In equation (3), the column vectors of  $\mathbf{N}$  form a basis of the linear space of parallel transformations. By definition, any parallel transformation can be obtained as a linear combination of those vectors. Figure 3 shows an example of basis for a simple quad mesh. The shaded regions correspond to strips where edge lengths are different from the initial mesh. Note that the three translations along X,Y,Z are also parallel transformations but preserve edge length and are not represented in Figure 3.

Practically, the sparse basis  $\mathbf{N}$  is computed for quadrilateral meshes using a propagation heuristic described in [10-11] (see Figure 4). This method defines the various parallel transforms decomposing the mesh into quadrangular patches and prescribing the edges length on two sides of the patches, one by one. The resulting basis of the linear space is not orthogonal, but its implementation and handling is relatively is for a designer.

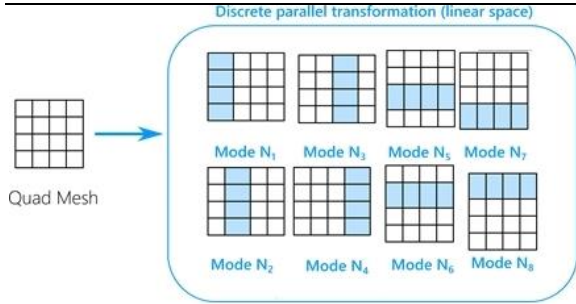


**Figure 3:** Visualisation of the linear space of possible parallel transformations for a 4x4 PQ-mesh (dimension of space is 4+4 with 3 translations).

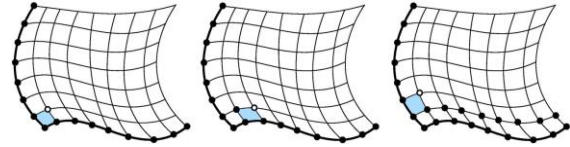


**Figure 4:** Heuristic for propagation of parallel transformation in a quadrilateral mesh [12] from the prescription of the lengths of the bold edges.

## 2.2 Alignment with mesh normals

Perhaps the most intuitive way to find an optimal offset is to try to fit the normals of the underlying shape. This is at least what the engineer's common sense advises: the optimal way to increase bending stiffness is to increase the thickness of the grid in the normal direction. So, depending on the modelling paradigm used, the designer has either access to a smooth surface (e.g. in NURBS modelling) or to a mesh (e.g. when performing mechanical form-finding). In this last case, one might for example define normals to a mesh based on the curvature tensor defined by Cohen-Steiner and Morvan [12].

For each vertex, we can thus define a unit normal: these normals can then be stored in a column vector  $\mathbf{V}$ . The best offset is simply found by performing an orthogonal projection of  $\mathbf{V}$  on the subset of possible torsion-free offsets. This procedure is illustrated for a polyline with two edges in Figure 5: the design input is shown in orange, whereas the basis of normal constructed with equation (3) is depicted in light blue.

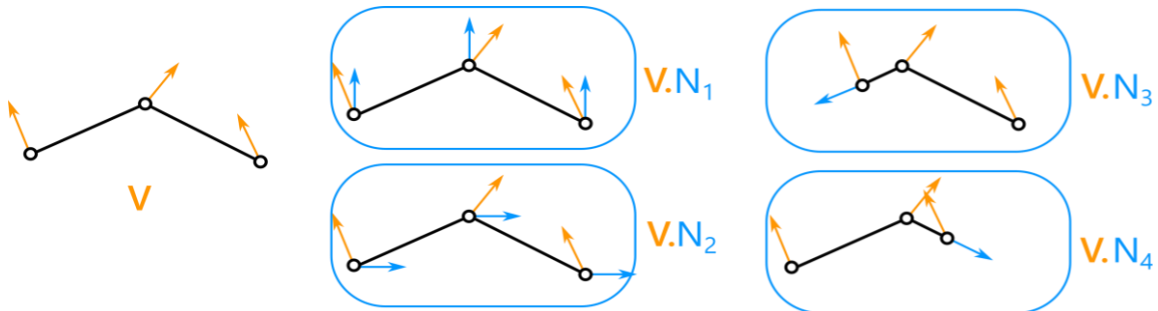


**Figure 5:** Projection of expected normals ( $\mathbf{V}$ , orange arrows) on the basis of the design space ( $\mathbf{N}$ , blue arrows)

With the notations of equation (3), noting that  $N_i$  corresponds to the  $i^{\text{th}}$  vector of the basis of nodal displacements, the optimal parallel transform is given by:

$$\mathbf{V}^* = \sum_i \langle \mathbf{V}_i | \mathbf{N}_i \rangle \cdot \mathbf{N}_i \quad (4)$$

The operation is done in linear time upon computation of the linear space of parallel transformations.

Note that other objectives than minimal deviation from surface normal could be also implemented such as constant face offset, alignment with specific direction for example (see detail in [13]). These last two constraints have been used indeed for the realization of a pavilion show in Boutillier *et al* [7].

### 2.3 What differential geometry tells us

On a smooth surface, the *geodesic torsion* of a curve with tangent vector  $t_1$  is the rate of rotation of the tangent plane of the surface along  $t_1$ . Figure 6 represents the interpretation of geodesic torsion: the curve is represented by a dashed line: the geodesic torsion measures how much the surface normal  $n_1$  rotates along  $t$  per unit length.

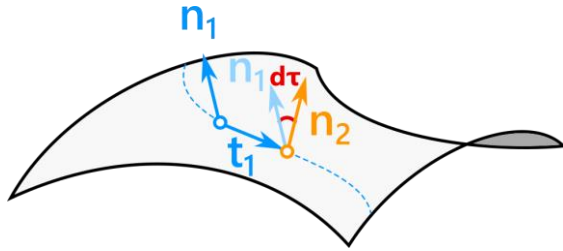


**Figure 6:** Geodesic torsion measures the rotation of the tangent plane of a surface (or its normal  $n$ ) upon unit displacement along the tangent vector of a curve  $t$ .

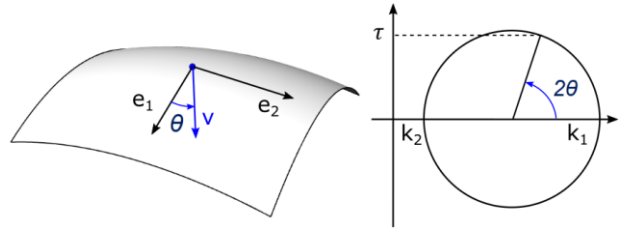


**Figure 7:** Mohr circle of curvature tensor

Geodesic torsion can be calculated using the principal curvature frame  $(e_1, e_2)$  [14] (Figure 7):

$$\tau = \frac{1}{2} \sin(2\theta) (k_2 - k_1) \quad (5)$$

Where:

- The geodesic torsion  $\tau$  is in a unit such as rad/m;
- $k_1, k_2$  are the principal curvature;
- $\theta$  is the angle between the direction of maximum curvature  $e_1$  and  $t_1$ .

This expression can be visualized using a Mohr circle, in the exact same way as a Mohr circle is used for plane stresses (see figure 7).

In the context of torsion-free structures constructed from parallel meshes, the goal of the discrete optimization problem is to fit the normal of the surface with torsion-free structure as well as possible. If we consider a polyline, this means that consecutive normals are coplanar, and thus that the normal surface should be developable (recall that developable surfaces can be defined as envelopes of planes). The only curves which satisfy this property are lines of curvature, because they have zero geodesic torsion. Indeed, in Figure 6, it seems obvious that the surface normals  $n_2$  and  $n_1$  are coplanar if and only if the angle  $d\tau$  (local geodesic torsion) is equal to zero.

We introduce  $\Phi(s_0)$  as the integral of geodesic torsion along the curve. It can simply be interpreted as the angle between the surface normal and the normal of the developable surface that was initially aligned with the surface normal at the start.

$$\Phi(s_0) = \int_{s_{min}}^{s_0} \tau ds \quad (6)$$

The optimal way to fit a developable surface along the normal is simply computed by finding the maximal (rightwards) and minimal (leftwards) value of  $\Phi$ . The minimal error possible between the normal of the surface and the rules of a developable surface going through the curve is thus given by equation (7).

$$\Delta\Phi = \frac{1}{2} (\max(\Phi) - \min(\Phi)) \quad (7)$$

Interestingly, this formula does not depend on the discretization, which is verified with numerical experiments.

## 2.4 Application

The projection technique has been applied to a surface based on the Berlin Hippo Haus (Figure 8). The maximal deviation from surface normals is  $15^\circ$ , and 90% of normal have a deviation from surface normal inferior to  $7^\circ$ . The reason for it is not only linked with the relevance of the method but also to the fact that the two domes are almost spherical surfaces where geodesic torsion is reduced for any curve.

One notes also that the distribution of angles is not very sensitive to the number of subdivisions, which can be understood by the smooth setting. Indeed, the maximal deviation with the surface normal is expected to be related to the integral of torsion of the curve. Figure 9 displays the distribution of deviation angles (the angles between the nodal axis and the surface normal) for two mesh densities.

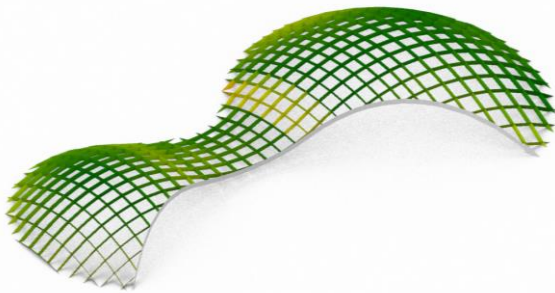


**Figure 8:** Torsion-free support structure for the Hippo Haus in Berlin. The mesh is based on a surface of translation, and is therefore not a curvature line network. The deviation between nodal axes and surface normal is inferior to  $15^\circ$ .

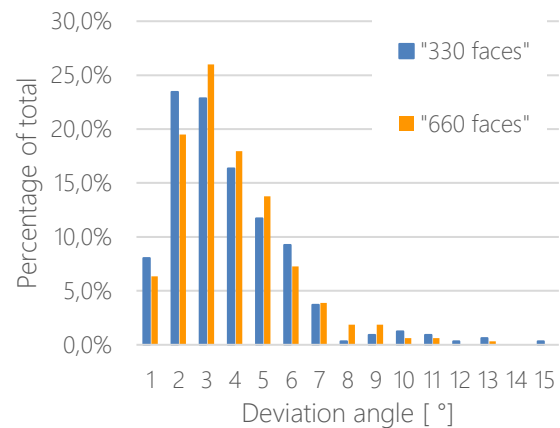


**Figure 9:** Distribution of deviation angle for two subdivisions of the Hippo Haus.

## 3. Case study

### 3.1 Practical implementation

As the mathematical theory of parallel meshes says that there exists a solution that minimizes the deviation from surface normal, it is worth searching for it with any optimization method: it will converge. Indeed, the practical implementation of the linear algebra methods described in previous section require the search of a basis of the null space which might seem tedious for many designers. On the contrary, many of them are used to work with geometric optimizers such as Kangaroo [15], ShapeUp [16] or equivalent... Practically, edge parallelism is a constraint which can easily be introduced within these tools. Coupling it with a constraint on the distance between two parallel edges and another constraint linked with the deviation from surface normal, one gets a simple set of three families of constraints whose weights can be adjusted so that the parallelism constraint is almost strictly satisfied. Computation time might be a little bit higher than using linear algebra, but the implementation time is close to zero. Practically on all the examples tested with Kangaroo by the authors, one gets a suitable parallel mesh in almost real time and results are in good agreement with the previously implemented method.

### 3.2 Reference mesh of the case study

The reference geometry of the case study is that of a pavilion constructed by Boutiller et al [7] and shown in figure 10. It has a complex grid geometry with many singularities in order to achieve i) proper alignment of the grid with free edges and ii) convergence of the grid toward the support. It is almost funicular from dead load and has 56 planar panels. It is made of wooden beams with rectangular cross sections  $45 \times 70 \text{ mm}$  forming a torsion-free layout. Their connections are achieved by 5mm plywood boxes (laser cut) which ensure the bracing of the structure as well. The polls at the four supports are built aligned with the structure tangent plane in order to minimize bending moments. The total covered area is close to 12 sqm with a maximum span of 4 m.

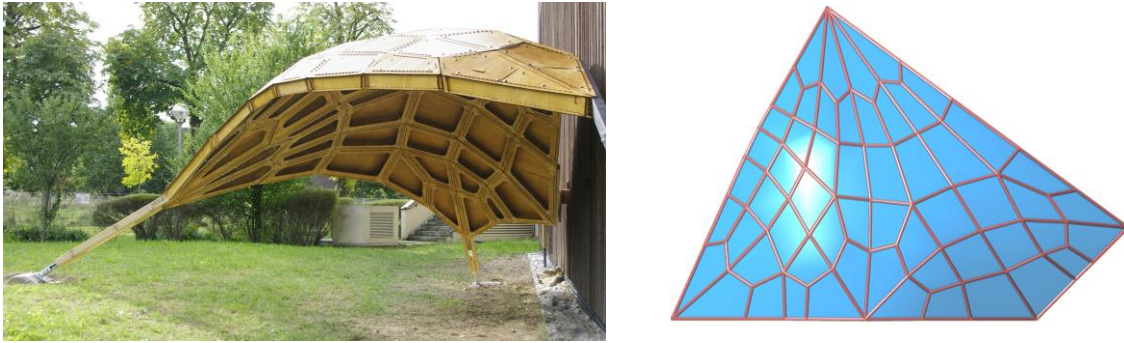


Figure 10: Side view of Boutillier *et al* pavilion [7] (left) with top view of the reference mesh (right)

### 3.3 Generation of the parallel mesh and comparison with offset mesh

In this section, two beam layouts are generated. In the first one, a parallel mesh minimizing the deviation from surface normal at a distance of approximately 100 mm from the reference mesh is computed. The corresponding beam layout is torsion free, as explained in previous section. In the second one, the beam planes are aligned with the bisecting planes of adjacent panels, they are thus aligned with surface normals but the resulting layout exhibits torsion at nodes. In the first model, the deviations of beam axes from surface normals range  $0^\circ$  to  $18.5^\circ$  with an average value of  $6.3^\circ$  (see figure 11 left). In the second model, the torsion at nodes (measured as the minimal cone angle containing beam midplanes intersections) range from  $0^\circ$  to  $5.9^\circ$  with an average value of  $2.1^\circ$  (see figure 11 right). In terms of fabrication constraint, note that a cone angle of  $0.57^\circ$  corresponds to a 1 mm distance between axes for a 100 mm beam. Therefore, if the layout with torsion at nodes should be built, one should be able to design a node that can accommodate size variation reaching up to 10 mm.

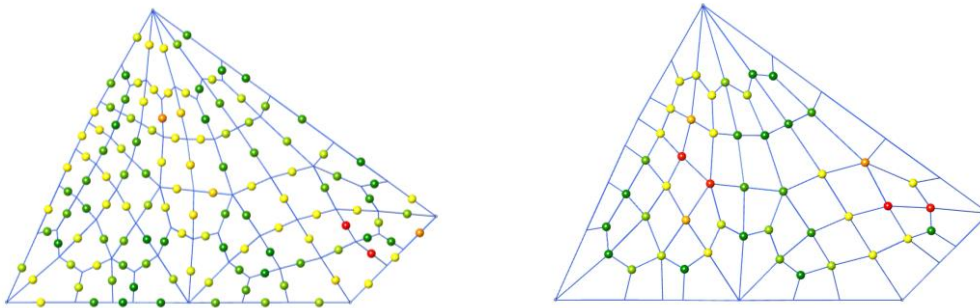


Figure 11: Deviation of the beam layout from ideal solution: (left) angular deviation of beams midplane from surface normal in the torsion free layout and (right) angular opening of the cone containing all midplane intersection in the layout with torsion at nodes. Minimal values are in green, maximal in red.

### 3.4 Influence on the mechanical behaviour

In this section, the two beam layouts are submitted to the same loading at nodes and their structural behaviour are compared with help of Karamba by just varying the local axes of the beams. In this case study, joints are supposed rigid which is not the case in the prototype but sufficient for the purpose of the present paper. If one considers the cross section used for the prototype (70x45), differences between the two layouts are negligible, in terms of displacements, stresses or critical buckling load. If one reduces the width of the cross sections to 4.5mm, then differences start appearing and the layout with torsion at nodes appears to underperform the torsion free layout of about 20% (see table 1). Looking at the forces in the structure, one observes that strong axis bending moments and normal forces are comparable in both layouts but that weak axis bending moments and torsion are 20% and 50% higher in the model with geometric torsion, respectively. Small axis eccentricities induced by nodal torsion causes hence additional deformations in the structure that one cannot neglect. Good fabrication properties hence go along with good mechanical performances.

It should be here noted that introducing the bracing provided by the plywood boxes cancels out the weak axis bending moments so that, in the braced configurations, the two layouts have again comparable performances.

**Table 1:** Comparison of max deflection, average normal forces and average bending moments, as well as critical buckling load for both beam layout for three configuration (i) with standard cross sections [70x45], (ii) with reduced cross sections [70x9], (iii) with reduced cross sections and bracing) structures. Values are given for a 100N load applied at each node.

	Layout	Disp_max [cm]	N_av [N]	M_av_y [N.m]	M_av_x [N.m]	M_av_z [N.m]	F_cr
Conf. 1 [70x45]	Torsion free	.091	309	9.8	1.9	8.2	58
	Normal	.091	307	9.7	1.9	8.7	58
Conf. 2 [70x4.5]	Torsion free	1.63	-355	15.6	0.3	3.5	0.12
	Normal	1.84	-355	15.6	0.3	4.2	0.36
Conf. 3 [70x4.5] +bracing	Torsion free	0.40	-268	5.8	0.1	0.0	0.87
	Normal	0.41	-267	5.8	0.1	0.1	0.86

#### 4. Conclusion

The design space of curved envelopes is strongly constrained when trying to obtain exact rationalization properties such as planar faces or torsion-free beam layout and node axes aligned with surface normal. In this article, we looked at how deviation from these strict constraints can increase the design freedom.

First a method that gives priority to torsion-free layouts and optimizes the nodal axes to fit surface normals was proposed. This method turns to a linear algebra minimization problem and proved to be computationally efficient. The quality of the results depends on the surface geometry and on the deviation of the layout from the principal curvature network.

Second, the influence of the beam layout in terms of deviation from surface normal and geometric torsion at nodes was investigated in a practical case study. It was found negligible in practical cases where the differences between strong axis inertia and weak axis inertia are not high. In the case of slender members, it was found that good mechanical properties go along with good fabrication properties. This interesting result should be further investigated on more examples.

#### References

- [1] X. Tellier, O. Baverel, C. Douthe, and L. Hauswirth, "Gridshells without kink angle between beams and cladding panels," *Proc. IASS Symp. 2018 Creat. Struct. Des. Boston, USA*, 2018.
- [2] H. Pottmann, Y. Liu, J. Wallner, A. I. Bobenko, and W. Wang, "Geometry of multi-layer freeform structures for architecture," *ACM Trans. Graph.*, vol. 26, no. 3, p. 65, 2007, doi: 10.1145/1276377.1276458.
- [3] Mesnil, R., Douthe, C., & Baverel, O. (2017). Non-standard patterns for gridshell structures: Fabrication and structural optimization. *Journal of the International Association for Shell and Spatial Structures*, 58(4), 277-286.
- [4] Y. Liu, H. Pottmann, J. Wallner, Y.-L. Yang, and W. Wang, "Geometric modeling with conical meshes and developable surfaces," *ACM Trans. Graph.*, vol. 25, no. 3, p. 681, 2006, doi: 10.1145/1141911.1141941.

- [5] Y.-L. Yang, Y.-J. Yang, H. Pottmann, and N. Mitra, “Shape Space Exploration of Constrained Meshes,” *ACM Trans. Graph.*, vol. 30, no. 6, 2011, doi: 10.1145/2070781.2024158.
- [6] X. Tellier *et al.*, “The Caravel heX-Mesh pavilion , illustration of a new strategy for gridshell rationalization,” *SN Appl. Sci.*, vol. 2, no. 781, 2020, doi: 10.1007/s42452-020-2561-2.
- [7] R. Boutillier, C. Douthe, L. Hauswirth, O. Baverel, Coupling grid topology generation and form-finding for architectural meshes adapted to support conditions, *Structures* 2024 (accepted)
- [8] R. Mesnil, C. Douthe, O. Baverel, and T. Gobin, “Form-finding of nexorades using the translations method,” *Autom. Constr.*, vol. 95, no. February, pp. 142–154, 2018, doi: 10.1016/j.autcon.2018.08.010.
- [9] R. Poranne, R. Chen, and C. Gotsman, “On Linear Spaces of Polyhedral Meshes,” *IEEE Trans. Vis. Comput. Graph.*, vol. 21, no. 5, pp. 652–662, 2015.
- [10] R. Mesnil, C. Douthe, O. Baverel, and B. Léger, “Morphogenesis of surfaces with planar lines of curvature and application to architectural design,” *Autom. Constr.*, vol. 95, pp. 129–141, 2018, doi: 10.1016/j.autcon.2018.08.007.
- [11] R. Mesnil, C. Douthe, O. Baverel, and B. Leger, “Marionette Meshes : Modelling free-form architecture with planar facets,” *Int. J. Sp. Struct.*, vol. 32, no. 3–4, pp. 184–198, 2017, doi: 10.1177/0266351117738379.
- [12] D. Cohen-steiner and J.-M. Morvan, “Differential geometry on discrete surfaces,” in *Effective Computational Geometry for Curves and Surfaces*, no. January, 2006, pp. 157–179.
- [13] X. Tellier, R. Mesnil, C. Douthe, O. Baverel, On the design of torsion free gridshells, accepted in the *Journal of IASS* (2024)
- [14] M. P. do Carmo, *Differential geometry of curves and surfaces*. Prentice-Hall, Inc., 1976.
- [15] D. Piker, Kangaroo: Form finding with computational physics, *Architectural Design*, Vol 83 (2), 136 – 137, 2013
- [16] S. Bouaziz, M. Deuss, Y. Schwartzburg, T. Weise, and M. Pauly, “Shape-Up : Shaping Discrete Geometry with Projections,” *Eurographics Symp. Geom. Process.*, vol. 31, 2012, doi: 10.1111/j.1467-8659.2012.03171.x.